Final Technical Report

STRUCTURE OF TURBULENCE IN THREE-DIMENSIONAL BOUNDARY LAYERS

Chelakara S. Subramanian

Florida Institute of Technology
150 W. University Boulevard
Melbourne, Florida 32901-6988
1993

Final Technical Report

STRUCTURE OF TURBULENCE IN THREE-DIMENSIONAL BOUNDARY LAYERS

Chelakara S. Subramanian

Aug-Nov 1993
NASA Grant No. NAG-1-1541

Florida Institute of Technology
150 W. University Boulevard
Melbourne, Florida 32901-6988

Table of Contents

Nomenclature

d	= diameter of the suction hole
m	= $-\rho_s V_s/\rho_e U_e$, suction ratio
Re_θ	= Reynolds number based on the momentum thickness and the edge velocity
U,W,V	= mean velocity components along x-, y- and z-directions, respectively
U_e,W_e	= mean velocity components at the edge of the boundary layer
V_1,V_2,V_3	= velocity components normal to the axis of beam-pairs 1, 2, and 3, respectively
V_s	= suction velocity
u,v,w	= fluctuating velocity components along x-, y- and z-directions, respectively
$\overline{u^2}$, $\overline{v^2}$, $\overline{w^2}$	= Reynolds normal-stress components along x-, y- and z-directions, respectively
$\overline{uv}$, $\overline{vw}$,$\overline{uw}$	= Reynolds shear-stress components along x-, y- and z-directions, respectively
u^*	= friction velocity
x, y, z	= streamwise, normal and transverse coordinates
α	= flow turning angle
β	= cross-flow angle between the external and local streamlines
β_w	= cross-flow angle, measured as the angle between the projected external streamline and the surface shear stress vector (limiting streamline)

δ = boundary layer thickness

ϕ = inclination of the laser-optics table to the horizontal plane

ν = kinematic viscosity

ρ_s, ρ_e = density of suction- and freestream air, respectively

θ = inclination of the beam-pair axis to the flow axis

$\Omega_x, \Omega_y, \Omega_z$ = mean vorticity components along x-, y- and z-directions, respectively

Abstract

This report provides an over view of the three-dimensional turbulent boundary layer concepts and, of the currently available experimental information for their turbulence modeling. It is found that more reliable turbulence data, especially of the Reynolds stress transport terms, is needed to improve the existing modeling capabilities. An experiment is proposed to study the three-dimensional boundary layer formed by a "sink flow" in a fully developed two-dimensional turbulent boundary layer. Also, the mean and turbulence field measurement procedure using a three-component laser Doppler velocimeter is described.

1. Introduction

By definition, a three-dimensional boundary layer has three non-zero mean velocity components that are functions of the three reference coordinates (x, y and z). The external potential velocity is a function of two coordinates (x, z) in the plane of the surface. If the external potential streamlines are straight lines which either converge or diverge then, as compared to a two-dimensional boundary layer there is only change in the boundary layer thickness and the velocity vector points in one direction throughout the boundary layer. On the other hand, if the potential streamlines are curved then, the imbalance between the decreasing centrifugal force (due to velocity reduction in the boundary layer) and the impressed radial pressure gradient force gives rise to secondary flow in the boundary layer with skewed velocity profiles as shown in Figure 1. This type of secondary flow is called by various names, such as, skew induced secondary flow (Prandtl's first kind of secondary flow-Bradshaw 1987), pressure-driven secondary flow (Anderson and Eaton 1989, Baskaran et al. 1990 etc.). In Figure 1, the x axis is chosen along the direction of the potential streamlines, z axis is orthogonal to x axis in the surface plane and y axis is chosen normal to the surface. Accordingly, the primary (U) component of velocity is the x-component, vertical (V) velocity is the y-component and secondary or cross-flow (W) component of the velocity is the z-component. Within the boundary layer centrifugal, viscous and convection effects are significant, but in the potential region only the centrifugal and convection effects are important. Therefore, if the sign of the lateral pressure gradient changes along external streamlines the corresponding cross-flow velocity changes tends to

lag behind and gives rise to a S-shaped cross-flow profiles some distance downstream of pressure gradient sign change. The velocity vectors within the boundary layer are non-collateral and therefore, the streamlines are skewed towards the concave side of the potential streamlines. The streamlines on the surface (also known as the limiting streamlines) have the maximum skew angles and the skew angle, in general, is a function of the y-distance normal to the surface. Also, the streamwise ($\partial U/\partial y$) and the cross-flow ($\partial W/\partial y$) velocity gradients give rise to mean streamwise vortices. Once this type of skew induced vortices are formed they are further diffused by viscous and Reynolds stresses.

There is a second kind of three-dimensional boundary layer that is typified by a *turbulent* flow in the rectangular corner or of a wing-body junction. Here, the streamwise mean vortices are created by shear stress gradients in both the y- and z- directions. These type of secondary flows are referred to as "stress induced secondary flow" or "secondary flow of Prandtl's second kind". Obviously, these vortices occur only in turbulent flows and, are, generally, weaker compared to the skew induced vortices.

2. Three-dimensional Boundary Layer Concepts

In three-dimensions generally we use a coordinate system that conforms to the surface (Body Fitted Coordinates), and this involves a network of two families of lines, not necessarily orthogonal, mapped over the surface plus the normals to the surface. Hence the curvature of the coordinates are introduced with associated centrifugal and coriolis terms in the equation as well as metrics of the system.

However, for small surface curvature, cartesian coordinates can be used for convenience. The boundary layer equations for the incompressible flow are given by

$$\rho\frac{DU}{Dt} = -\frac{\partial p}{\partial x} + \frac{\partial \tau_{xy}}{\partial y}$$

$$\rho\frac{DW}{Dt} = -\frac{\partial p}{\partial z} + \frac{\partial \tau_{zy}}{\partial y},$$

$$\frac{\partial U}{\partial x} + \frac{\partial V}{\partial y} + \frac{\partial W}{\partial z} = 0$$

where, $\tau_{xy} = \mu \frac{\partial U}{\partial y}$ and $\tau_{zy} = \mu \frac{\partial W}{\partial y}$ for laminar flows

and, $\tau_{xy} = \mu \frac{\partial U}{\partial y} - \rho\overline{uv}$ and $\tau_{zy} = \mu \frac{\partial W}{\partial y} - \rho\overline{wv}$ for turbulent flows

$\partial p/\partial y$ is assumed negligible and, $\partial p/\partial x$ and $\partial p/\partial z$ are known from the potential flow solution. In turbulent flows, the U-component motion is governed by $\partial \overline{uv}/\partial y$ and the W- component is governed by $\partial \overline{vw}/\partial y$. In certain flows the term $\partial \overline{uw}/\partial x$, omitted from the above equation, may also be significant. The three-dimensional Navier-Stokes equation are elliptic, which means that information from a point can be propagated by convection, viscous diffusion, or pressure variations. Under the three-dimensional boundary layer approximations the influence of the solution at one point is transfered to other downstream points within a wedge-like region formed by the surface streamline (actually surface shear stress vector) and the free streamline by viscous diffusion in the vertical direction and by convection in the streamwise/cross-stream directions. This region is called "domain of influence" as indicated in the Figure 2. On the other hand, the solution at a given point depends on the solution in another upstream wedge-like region called the "domain of dependence". Also, in three-dimensional boundary layers streamwise vortices, Ω_x, are generated, as given by the following vorticity transport equation, by; (i) quasi-inviscid deflection of existing mean vorticity Ω_y and Ω_z by the mean velocity gradients and, (ii) turbulent stress gradients.

$$U\frac{\partial \Omega_x}{\partial x} + V\frac{\partial \Omega_x}{\partial y} + W\frac{\partial \Omega_x}{\partial z} = \Omega_x \frac{\partial U}{\partial x} + \Omega_y \frac{\partial U}{\partial y} + \Omega_z \frac{\partial U}{\partial z} + \left(\frac{\partial^2}{\partial y^2} - \frac{\partial^2}{\partial z^2}\right)\left(-\overline{vw}\right) + \frac{\partial^2}{\partial y \partial z}\left(\overline{v^2} - \overline{w^2}\right) + \nu\nabla^2\Omega_x \qquad \text{.....(1)}$$

For the purposes of analysis, three-dimensional boundary layers are classified in to three categories; *thin shear layers, slender shear flow*, and *three-dimensional shear flow.*

2.1 Thin shear layer

In thin shear boundary layer flows, $\partial/\partial y >> \partial/\partial x \sim \partial/\partial z$ when operating on any velocity component. These correspond closely to two-dimensional boundary layers and sometimes called boundary

sheets. Here, V is small compared to U and W and the pressure is constant in the y-direction. Such flows occur on yawed flat plate, finite wings and propeller blades, except in the region near the root and tip. Three-dimensional thin shear layers have been solved in specific cases using some further simplifying assumptions. These are; (i) the "independence principle" according to Prandtl (1946), (ii) the infinite swept wing or infinite yawed cylinder and (iii) the "small cross flow assumptions" or the "principle of prevalence".

In the case of thin shear layers, with negligible viscous diffusion in the x- and z-directions the information is propagated in the cross-flow plane only by convection at an angle $\tan^{-1}(W/U)$. According to the independence principle the velocity in the boundary layer which is parallel to the wall is also parallel the potential flow at all points, or in other words, $W/U = W_e/U_e$. This is valid for a yawed flat plate boundary layer. This causes the boundary layer thickness of a turbulent boundary layer on a yawed flat plate (e.g. Ashkenas and Riddel 1955) grow faster in the downstream direction than with an unyawed plate. But, the independence principle can be applied to laminar flows only, because in turbulent flows there is a strong interaction between the spanwise and chordwise components of the velocity fluctuations which change the mean velocities.

For infinite swept wing or infinite yawed cylinder conditions, the z-derivative is zero and the surface is assumed to be developable (one that can be obtained by rolling up a plane flexible sheet). The calculation methods for this case is provided by Adams (1975), Krause (1974) and Cebeci (1974).

The "small cross-flow" or the "principle of prevalence" assumption amounts to assuming that W is so small that it may be ignored in the momentum equation for U. Generally, small cross-flow assumption holds good in turbulent boundary layers to cross-flow angles, β_w, smaller than six degrees. In flows which have a plane of symmetry some further simplifications are possible with small cross-flow assumption. For example, Nash and Patel(1972) assumed the cross-flow mean velocity as well as the shear stress, $\rho\overline{vw}$, to vanish whereas the gradients in the z-direction are retained for their three-dimensional boundary layer with a plane of symmetry. A more detailed discussion of the turbulent flow at a plane of symmetry are available in Johnston (1960) and Pierce(1963).

2.2 Slender shear flow

This is the kind of shear flow along corner walls, where $\partial/\partial y$,

$\partial/\partial z \gg \partial/\partial x$. The shear stress gradients in both y- and z-directions are important in the Reynolds stress equations. This can give rise to discrete streamwise vortices in the boundary layer as described above (*cf.* equation 1).

2.3 Three-dimensional shear flow

The third category is called *three-dimensional shear flow*, where $\partial/\partial x \sim \partial/\partial y \sim \partial/\partial z$. This needs higher order boundary layer equations with term-by-term modeling of Reynolds stresses, or the full Navier-Stokes equations.

Detailed reviews of all the above three kinds of three-dimensional flows may be found in; Cooke and Hall (1962), Joubert et al. (1967), Sherman (1968), Wheeler and Johnston (1972,1973), Nash and Patel (1972), Blottner (1975), Horlock et al. (1966), Fernholz (1982) and Eichelbrenner and Oudart (1955).

3. Previous experiments in three-dimensional turbulent boundary layer flows

A few experimental results are available for three-dimensional thin shear layers: on pressure-driven secondary flows on swept wings by Etheridge (1971), van den Berg et al. (1975) and Elsenaar and Boelsma (1974); on curved channel flows by Klinksiek and Pierce (1970), Vermeulen (1971) and ship hulls by Larsson (1975). Experiments on shear-driven secondary flows are even fewer; Bradshaw and Terrell (1969), Crabbe (1971) and Driver and Hebbar (1985). But in all the measurements, no accurate turbulence data in the vicinity of the wall is available.

3.1 Mean flow data

Bradshaw (1987) considered the effects of imposing a spanwise pressure gradient on a two-dimensional boundary layer that lead to a three-dimensional flow. Here, the spanwise pressure gradient (albeit small) is created as a result of changes in the radius of curvature of streamlines as the flow passed over a curved section. The streamlines at radii greater than the mean radius experience lower streamwise velocities and the streamlines at radii smaller than the mean radius experience higher streamwise velocities. This spanwise velocity gradient ($\partial U/\partial z$) gives rise to a streamwise vorticity component, Ω_x, by laterally skewing the pre-existing spanwise vorticity vector, Ω_z (predominantly $-\partial U/\partial y$). The axial

vorticity created this way has mostly contributions from $\partial W/\partial y$ as $\partial V/\partial z$ is significantly small, at least initially. For small flow deflection angles α, we have the Squire Winter Hawthorn (SWH) secondary flow formula, $d(\Omega_x/\Omega_z)/dx = d(W/U)/dx$ or $2\alpha = -\tan^{-1}(W/U)$, which implies that vortex lines are skewed through an angle equal and opposite to that through which the flow has turned. This relation is found to agree reasonably well with the experiments (e.g. Bradshaw and Pontikos 1985, Driver and Hebbar 1985) for the external streamlines. However, close to the surface the flow deflection angles are smaller than SWH predictions. According to Bradshaw (1987), when the sign of the spanwise pressure gradient changes further downstream a crossover profile in W component may occur. It is difficult to fit crossover profiles by means of simple relations. For non-crossover profiles Johnston (1960) proposed a correlation model for a composite velocity defined as $U/\cos\beta_w$ as,

$$\frac{U}{u^* \cos\beta_w} = \frac{1}{\kappa}\ln\left(\frac{yu^*}{\nu}\right) + C$$

Here, u^* is the friction velocity formed with total shear stress, and β_w is the difference between the direction of the velocity vector in at the outer edge of the boundary layer and the skin friction vector at the wall. Among several other mean velocity models for Mager's (1952) relation,

$$\frac{W}{U} = \left(1-\frac{y}{d}\right)^2 \tan(\beta_w),$$

seems to provide the best agreement with experiments.

3.2 Turbulence data

Turbulence data are available for a variety of three-dimensional boundary layer flows including pressure-driven secondary flow, vortex imbedded boundary layer flow and cross-stream wall jets . These results are discussed now. The turbulence results of Bradshaw and Pontikos (1985), from their study on infinite swept wing, indicate some interesting behavior: (i) the ratio of the magnitude of the resultant turbulent shear stress to the turbulent kinetic energy drops rapidly as the cross flow velocity component increases, (ii) the development of the secondary shear stress, $\rho\overline{vw}$ is

slower than the development of cross-flow velocity W and its gradient $\partial W/\partial y$, and (iii) the viscous dissipation is larger than would be for a two-dimensional flow. Overall, the turbulent activity was decreased by the cross-flow, leading to reductions in turbulent transport of momentum, turbulent energy and turbulent shear stress across the layer. The explanation is that the large eddies in the initial two-dimensional flow are tilted sideways by the cross-flow velocity gradient, and this tilting reduces the capacity of the eddies to transport the above three turbulent quantities in the transverse direction. However, the pressure-strain" redistribution terms and the turbulent transport terms in the Reynolds-stress transport equations may still respond immediately to the $\partial U/\partial y$ and $\partial W/\partial y$ gradients. Anderson and Eaton (1986) also noticed similar effects on flow around surface mounted obstacles

In the 1982 Eurovisc Workshop, existing turbulent models and calculation methods have been evaluated for predicting flow on infinite swept wing. The general consensus is that no single model or calculation methods provide satisfactory predictions of all the flow quantities, particularly in the near wall regions. It is also deliberated that detailed turbulence measurements in the sublayer are scarce and models have to be adjusted to yield the right mean velocity profile.

If the lateral deflection of the vortex line is confined to only small spanwise distance, then concentrated longitudinal vortices are formed. For example, the trailing vortices created by the leading edge of a slender wing. These vortices can be isolated vortices (e.g. Gad-el-Hak and Blackwelder 1985, Cutler and Bradshaw 1986) in inviscid flow or they can be embedded in the boundary layer (e. g. Shabaka et al. 1985, Westphal et al. 1985, Eibeck and Eaton 1985, Mehta and Bradshaw 1986 and Subramanian et al. 1993). Cutler and Bradshaw's (1986) studies show that in the core of the isolated vortex the turbulent mixing is small yet, longitudinal turbulence intensity values are significant due to the presence of longitudinal waves. Since turbulence production per say is absent, a Reynolds stress model which works well for truly turbulent flows may not work for this case (e.g. Majumdar and Rodi 1985).

Concentrated vortices from an oncoming boundary layer are generated in junction flows of a wing, a turbomachinery blade, or a building. If the leading edge is sharp, the concentrated vortices may be close enough to surface to be rapidly diffused by viscous or Reynolds stresses. A detailed investigation of turbine-blade junction flow has been done by Langston et al. (1977) and Langston (1980),

but complete turbulence data is not available. Shabaka and Bradshaw (1981) have reported results of turbulence measurements on a simplified wing body junction flow. Here one can evidence the formation of pairs of stress induced vortices following the initial formation of pressure-driven horse-shoe vortices, as shown by Nakayama and Rahai (1984).

The general consensus is that for both corner vortex as well as embedded vortex flows even the most refined turbulence models do not give adequate predictions of the cross-stream intensities and secondary shear stresses that control the diffusion of streamwise vorticity. Probably, an improved modeling of the pressure-strain term in the Reynolds transport equation is necessary.

Flows in curved channels and ducts develop secondary flow (and longitudinal vortices) due to centrifugal instability. Although these vortices are weaker than the junction- and embedded vortices (Subramanian et al. 1992) they can change the turbulence structure. Longitudinal surface curvature tends to stabilize the turbulence near the inner wall and destabilize that near the outer wall. The most recent detailed turbulent measurements are by Chang et al. (1983) in a squared curved duct and Azzola and Humphrey (1984) in a curved pipe. But these measurements do no include secondary shear stress or triple product data. Unfortunately, the yz-plane shear stress, $\rho\overline{vw}$, is an essential part of the streamwise vorticity generation (*cf.* equation 1).

The most spectacular stress induced secondary flows are found in three-dimensional jets and wall jets. In this case there is a strong interaction between the mean flow and the turbulent stresses. As shown by Launder and Rodi (1983) for a three-dimensional wall jet, stress induced vortices play as much important role as the skew-induced vortices in the dynamics of motion.

4. Proposed experiment: *On the structure of turbulence in a "sink flow"*

The above review suggests that for modeling three-dimensional turbulent boundary layers flows of engineering interest, we still lack the complete understanding of the relation between the three-dimensional mean flow and the turbulence structure. The main question is the behavior of $\overline{vw}$ due to the mean flow interaction. Conventional measurements of $\overline{vw}$ (e.g. Andreopolous and Rodi 1984, Shayesteh et al. 1985) using hot-wire anemometry have calibration problems due to subtraction of two cross-wire

readings. Reynolds transport equation for this shear stress component involve pressure strain-rate product term which is also difficult to measure with reliable accuracy. The proposed experiment is aimed at a thorough investigation of mean and turbulent fields and their interactions in a boundary layer flow using a three-component laser Doppler velocimeter.

4.1 Experimental setup

The experiments are to be conducted in the 20" X 28" Shear Flow Wind Tunnel facility of Experimental Flow Physics branch at the NASA Langley Research Center (LaRC). This tunnel has a rectangular test section, 0.51 m X 0.71 m, and 4.57 m long and can produce velocities of up to 46 m/s. At a free stream speed of 20 m/s the freestream turbulence intensity is less than 0.08 percent (Subramanian 1992). A splitter plate with a semi-elliptic leading edge can be used as the test surface. The tunnel pressure gradient can be adjusted by adjusting the tunnel upper wall.

A three-dimensional boundary layer can be created by introducing suction at a streamwise location x = 3.67 m from the leading edge in a nominally two-dimensional turbulent flat plate boundary layer. The experiments are to be performed at a Reynolds number based on the momentum thickness, Re_θ, of about 8100 so that the turbulence is fully developed and has broad band spectrum of distinguishable length scales. Boundary layer suction can created by drawing air with a suction/vacuum pump through a 1 cm diameter hole (d) at the center line of the plate. At the location of the hole the canonical boundary layer thickness, δ, is estimated to be about 6.2 cm. Thus the ratio d/δ will be about 0.16. The magnitude of the suction can be varied so that the ratio of suction mass flux to the free stream mass flux, $-\rho_s V_s/\rho_e U_e$, called suction ratio m, is in the range 0.5-1.5. For this range the flow through the suction duct should be laminar for U_e = 20 m/s. At lower suction ratios, only the near-wall region of the boundary layer will probably be affected, but at higher ratios the entire boundary layer is expected to be altered. The "sink flow" created by the suction is meant to introduce the additional, V and W velocity components in the flow, particularly near the wall. The three mean velocity components, six Reynolds stresses and ten Reynolds triple products (contributing to turbulent transport) can be measured using a three-component laser Doppler velocimeter described below. These measurements should provide us an insight as to how the turbulence structure (especially in the near-wall region) changes in a sink flow.

4.2 LDV measurement

The LDV system: As mentioned above, for measuring velocities a three-component, Argon-ion laser Doppler velocimeter is to be used. A LDV system has been developed and being used by Dr. J. T. Kegelman and his associates at EFPB. This system consists of a COHERENT Innova 90, 5-Watt Argon-ion, water-cooled laser, THERMO SYSTEMS, INC., (TSI) transmitting and receiving (photo-multiplier tubes) optics for violet (476.5 nm), blue-green (496.5 nm) and green (514.5 nm) colored beams, TSI frequency shifter and MACRODYNE, INC. signal processing unit. For traversing the probe volume, a KLINGER three-axis micro-traverse control that allows micrometer movement, is used. The signal processing and traversing can be automated using the AEROMETRICS Doppler Signal Analyzer software.

In any turbulence measurement the probe resolution and accuracy are important factors. By using a 600 mm lens with a beam separation of 50 mm we can obtain an average probe-volume diameter of about 120 μm and a length of about 800 μm. Although, a subminiature hot wire probe perhaps can provide a better spatial resolution, the LDV is preferable from the point of view of non-intrusive probing capabilities and not requiring a precalibration. But several past studies (e. g. Driver and Hebbar 1985) show that LDV measurements are not devoid of problems. For example, non-uniform particle seeding can not only slow down the data rate but also can give rise to other problems such as multiple seeds in the probe-volume at a given time and signal cross-talks (for 2- and 3-component LDV). Also, if the beam-pair crossings are non-coincident at the probe-volume that will cause velocity bias errors. The errors due to these problems can be minimized by careful beam alignment and by controlling particle seeding. For air, 2 μm diameter polystyrene latex microspheres are good for seeding. In the setup shown in Figure 4, the three different color beam pairs intersect (non-orthogonally) at the same point in space. The beam pair 1 (voilet) is oriented at $-55(=\theta_1)$ degrees to the flow axis, the beam pair 2 (blue-green) normal to the flow axis and the beam pair 3 (green) at $+55(=\theta_3)$ degrees to the flow axis. Then, simultaneous measurements of all three velocities can be made. The measured velocities (V_1, V_2, V_3) with respect to the beam axes are then transformed into cartesian velocity components (U, V, W) before performing the ensemble averaging. The transformation matrix is,

$$\begin{bmatrix} V_1 \\ V_2 \\ V_3 \end{bmatrix} = \begin{bmatrix} U \\ V \\ W \end{bmatrix} \begin{bmatrix} \cos\theta_1\cos\phi & 0 & \sin\theta_1\cos\phi \\ 0 & \cos\phi & 0 \\ \cos\theta_3\cos\phi & 0 & \sin\theta_3\cos\phi \end{bmatrix}.$$

The optics table has a small dip angle of about 10 (=ϕ) degrees with respect to horizontal plane in order to facilitate measurements very close to the wall.

Velocity Survey Map: Velocity measurements are proposed around the suction hole over an area covering 1.5 diameters upstream to 1.5 diameters downstream from the hole center and, 1.5 diameters on either sides from the hole center (see Figure 5). An uniform traverse step size of 0.2 diameter can be used in both x- and z- directions, amounting to 225 probe locations per horizontal plane. In the normal direction, about 40 non-uniformly spaced heights can be used to cover the entire boundary layer. The smallest height corresponding to the probe-volume semi-diameter is about three viscous units at a freestream velocity of 20 m/s. Therefore, we can probe even within the linear sublayer.

5. Summary

This report provides an over view of the three-dimensional turbulent boundary layer concepts and the existing turbulent modeling information. It is concluded that the existing turbulence models fall short of accurately predicting boundary layers with strong secondary flows, especially when turbulent stress interactions also occur. In particular, to model the generation of shear stress induced streamwise vortices we need a better understanding of the behavior of Reynolds stresses and pressure strain-rates in three-dimensional flows. Here, a method is suggested using suction to create a three-dimensional boundary layer in a fully developed two-dimensional turbulent boundary layer. Since the surface boundary condition is altered, the changes to the turbulence structure corresponding to the changes in the mean motion is expected to be immediate. A non-intrusive, mean and turbulence field measurement using a three-component laser Doppler anemometer is prescribed.

6. Acknowledgement

This work is funded by the NASA Research Grant NAG-1-1541.

The author is very grateful to Drs. Steve Robinson and Mike Walsh of EFPB for their encouragement and support for this project.

7. References

Adams, J. C. Calculation of compressible turbulent boundary layers on an infinite yawed airofoil, *J. Spacecraft*, 12, 1975, p. 131

Ahkenas, H. and Riddel, F. R. Investigation of the turbulent boundary layer on a yawed flat plate, *NACA TN* 3383, 1955

Anderson, S. D. and Eaton, J. K. Experimental study of pressure-driven three-dimensional turbulent boundary layer, *AIAA* paper 86-0211, 1989

Andreopolous, J. and Rodi, W. Experimental investigation of jets in a cross-flow, *J. Fluid Mech.* 138, 1984, p. 93

Azzola, J. and Humphrey, J. A. C. Developing turbulent flow in a 180° curved pipe and its downstream tangent. *Rept. LBL-17681*, Lawrence Berkeley Lab., Calif., 1984

Baskaran V., Pontikis, Y. G. and Bradshaw, P. Experimental investigation of three-dimensional turbulent boundary layers on "infinite" swept curved wings, *J. Fluid Mech.* 211, 1990, p.95

Blottner, F. G., Computational techniques for boundary layers: in E. Krause, computational methods for inviscid and viscous two- and three-dimensional flow field, *AGARD- LS-* 73, 1975, p. 3-1

Bradshaw P. and Pontikos, N. Measurement in the turbulent boundary layer on an "infinite" swept wing, *J. Fluid Mech.* 159, 1985, p. 105

Bradshaw P. and Terrell, M. G. The response of a turbulent boundary layer on an infinite swept wing to the sudden removal of pressure gradient, *NPL Aero. Rept.* 1305, 1969

Bradshaw, P. Turbulent secondary flows, *Ann. Rev. Fluid Mech.*, 19, 1987, p. 53

Cebeci, T. Calculation of three-dimensional boundary layers I, swept infinite cylinders and small cross flow, *AIAA J.*, 12, 1974, p.779

Chang, S. M., Humphrey, J. A. C., Johnston, R. W. and Launder, B. E. Turbulent momentum and heat transport in flow through a 180° bend of square cross-section, Presented at *Int. Sympo. Turbulent Shear Flow*, 4th, Karlsruhe, 1983

Cooke, J. C. and Hall, M. G. Boundary layers in three-dimensions, *Prog. Aero. Sci.* 2,1962, p. 221

Crabbe, R. *Rept. 71-2*, Mech. Engng. Dept., McGill Univ., 1971

Cutler, A. D. and Bradshaw, P. The interaction between a strong

longitudinal vortex and a boundary layer, *AIAA* paper 86-1071, 1986

Driver, D. M. and Hebbar, S. K. Experimental study of a three-dimensional, shear driven, turbulent boundary layer using a three-dimensional laser Doppler Velocimeter, *AIAA* paper 85-1610, 1985

Eibeck, P. and Eaton, J. Heat-transfer effects of a longitudinal vortex imbedded in a turbulent boundary layer, *Rep.* Dept. Mech. Engng., Stanford Univ.,1985

Eichelbrenner, E. A. and Oudart, A. Method de calcul de la couche limite tridimensionelle. Application a un corps fusel incline sur le vent. *ONERA pub.* 76, Chatillon, 1955

Elsnaar, A. and Boelsman, S. H. Measurement of the Reynolds stress tensor in a three-dimensional turbulent boundary layer under infinite swept wing conditions, *NLR TR*-74095U, Amsterdam, 1974

Etheridge, D. W. *Ph. D. thesis*, Queen Mary College, London, 1971

Fernholz, H. H. in Krause, E. *Three-dimensional turbulent boundary layers*, Berlin, Springer-verlag, 1982, p. 389

Gad-el-Hak, M. and Blackwelder, R. F. The discrete vortices from a delta wing, *AIAA J.* 23, 1985, p. 961

Horlock, J. H., Norbury, J. F. and Cooke, J. C. Three-dimensional boundary layers: a report on Euromech 2, *J. Fluid Mech.* 27,1966, p. 369

Johnston, J. P. On three-dimensional turbulent boundary layers generated by secondary flow, *Trans. ASME* 82D, 1960, p. 233

Johnston, J. P. The turbulent boundary layer at a plane of symmetry in a three-dimensional flow,*Trans. ASME* 82D, 1960, p. 622

Joubert, P. N., Perry, A. E. and Brown K. C.: In: *Fluid Mechanics of Internal Flow*, Sovran, G. (Ed.) , Elsevier, Amsterdam, 1967

Klinksiek, W. F. and Pierce, F. J. Simultaneous lateral skewing in a three-dimensional turbulent boundary layer flow, *Trans. ASME* 92D, 1970, p. 83

Krause, E. *Int. Congr. Aerospace Sci. Paper*, 74-20, 1974

Langston, L. S. Crossflows in a turbine cascade passage, *Trans. ASME, J. Engng. Power*, 102, 1980, p. 866

Langston, L. S., Nice, M. L. and Hooper, R. M. Three-dimensional flow within a turbine cascade passage, *Trans ASME, J. Engng. Power* 99, 1977, p. 21

Larsson, L. *Ph. D. thesis*, Chalmers Univ., Goteborg, 1975

Launder, B. E. and Rodi, W. The turbulent wall jet- measurements and modeling, *Ann. Rev. Fluid Mech.* 15, 1983, p. 429

Mager, A. Generalisation of the boundary layer momentum integral equations to three-dimensional flows including those of a rotating system, *NACA Rept* 1067, 1952

Mehta, R. D. and Bradshaw, P. Longitudinal vortices imbedded in turbulent boundary layers, Part II. Vortex pair with "common flow" upwards, *J. Fluid Mech.* 188, 1988, p. 529

Majumdar, S. and Rodi, W. Numerical calculations of turbulent flow past circular cylinders. Presented at Symp. Numer. And Phys. Aspects of Aerodyn. Flows, 3rd, Long Beach, Calif., 1985

Nakayama, A. and Rahai, H. R. Measurement of turbulent flow behind a flat plate mounted normal to the wall, *AIAA J.* 22, 1984, p. 1817

Nash J. F. and Patel, V. C. *Three-Dimensional Turbulent Boundary Layers*, SBC Technical Books, Atlanta 1972

Prandtl, L. On boundary layers in three-dimensional flow, *Min. Aircraft Production (Volkenrode) Repts. and Trans.* 64, 1946

Schlichting, H. *Boundary Layer Theory*, New York, McGraw-Hill, 1979

Schetz, J. A. *Boundary Layer Analysis*, Prentice Hall, New Jersey, 1993

Shayesteh, M. V., Shabaka, I. M. M. A. and Bradshaw, P. Turbulence structure of a three-dimensional impinging jet in a cross stream, *AIAA* paper 85-0044, 1985

Shabaka, I. M. M. A. and Bradshaw, P. Turbulent flow measurements in an idealized wing/body junction, *AIAA J.* 19, 1981, p. 131

Shabaka, I. M. M. A., Mehta, R. D. and Bradshaw, P. Longitudinal vortices imbedded in turbulent boundary layers. Part I. Single vortex, *J. Fluid Mech.* 155, 1985, p. 37

Sherman, F. S. *Rept. RM-4843-Pr*, Rand Corp., Santa Monica 1968

Subramanian, C. S. A study of flow past a rotating disk, *Summer Faculty Research Rept.* ICASE, NASA LaRC, 1992

Subramanian, C. S., Ligrani, P. M. and Tuzzolo, M. F. Surface heat transfer and flow properties of vortex arrays induced artificially and from centrifugal instabilities, *Int. J. Heat and Fluid Flow 3*, 1992, p. 210

Subramanian, C. S., Ligrani, P. M., Green, J. and Donner, W. D. Turbulence structure of embedded-vortex/wall-jet interaction in a turbulent boundary layer, *in preparation*, 1993

van den Berg, B., Elsenaar, A., Lindhout, J. P. F. and Wesseling, P. J. Measurements in an incompressible three-dimensional turbulent boundary layer, under infinite swept-wing, conditions, and comparison with theory, *J. Fluid Mech.* 70, 1975, p. 127

Vermeulen, A. J. *Ph. D. thesis*, Univ. of Cambridge, 1971

Westphal R. V., Eaton, J. K. and Pauley, W. R. Interaction between a vortex and a turbulent boundary layer in a streamwise pressure gradient, in *Turbulent Shear Flows* 5, Berlin, Springer-Verlag 1985

Wheeler, A. J. and Johnston, J. P. Rept. MD-32, Dept. Mech. Engng., Stanford Univ. 1972

Wheeler, A. J. and Johnston, J. P. An assessment of three-dimensional turbulent boundary layer prediction methods, Trans. ASME 951, 1973, p. 415

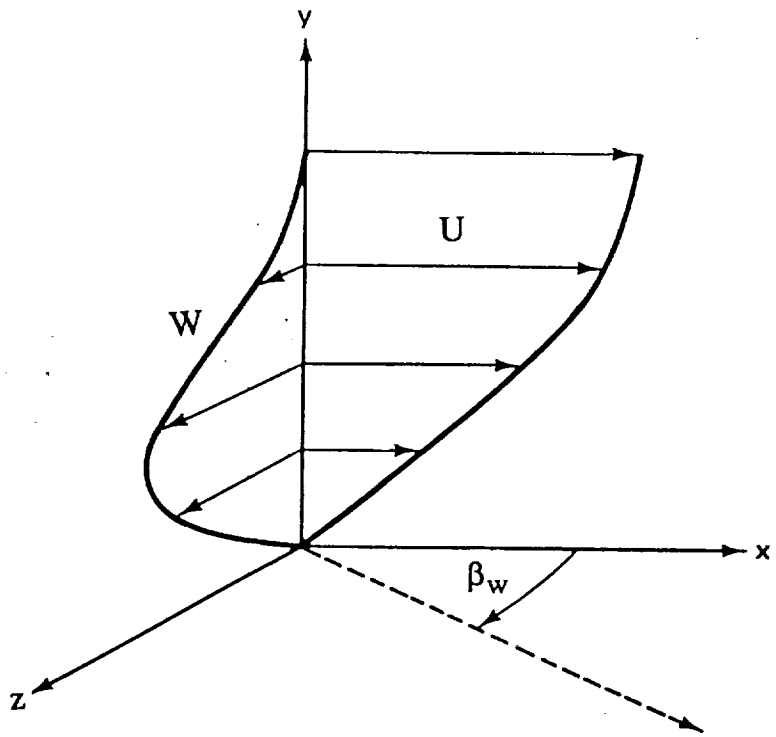

Figure 1. Typical velocity profile shape in a pressure-driven three-dimensional boundary layer.

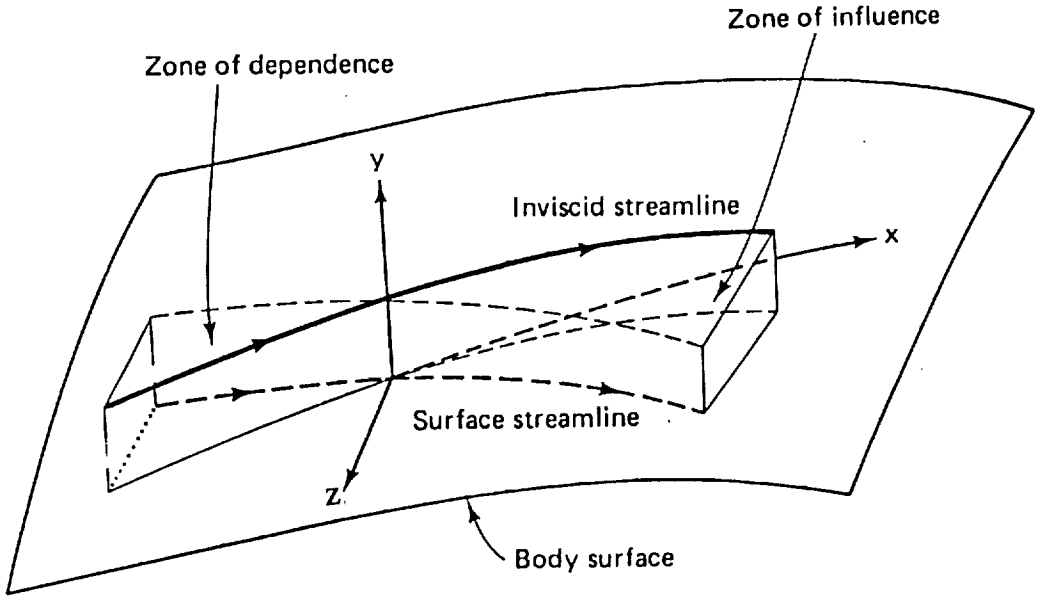

Figure 2. Regions of influence and dependence in a three-dimensional boundary layer.

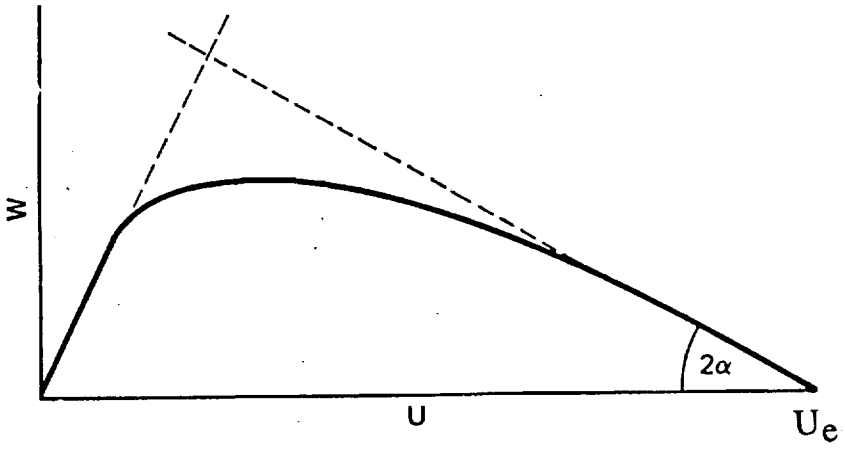

Figure 3. Gruschwitz-Johnston polar plot of W vs. U in streamline coordinates.

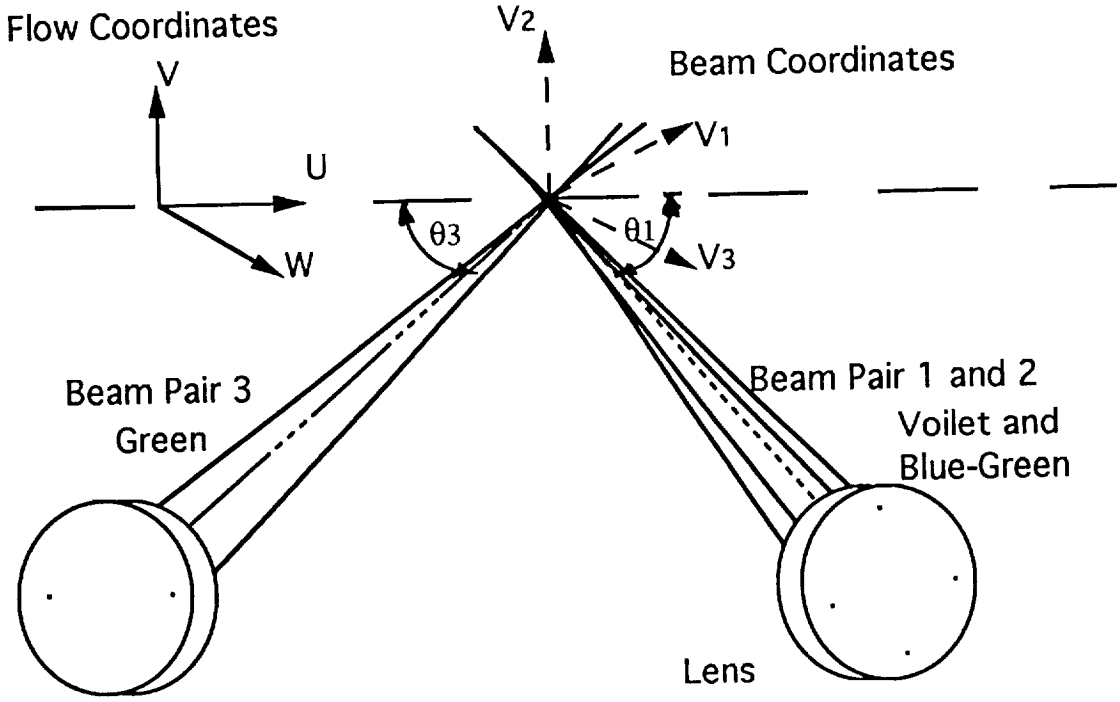

Figure 4. Three-component LDV configuration.

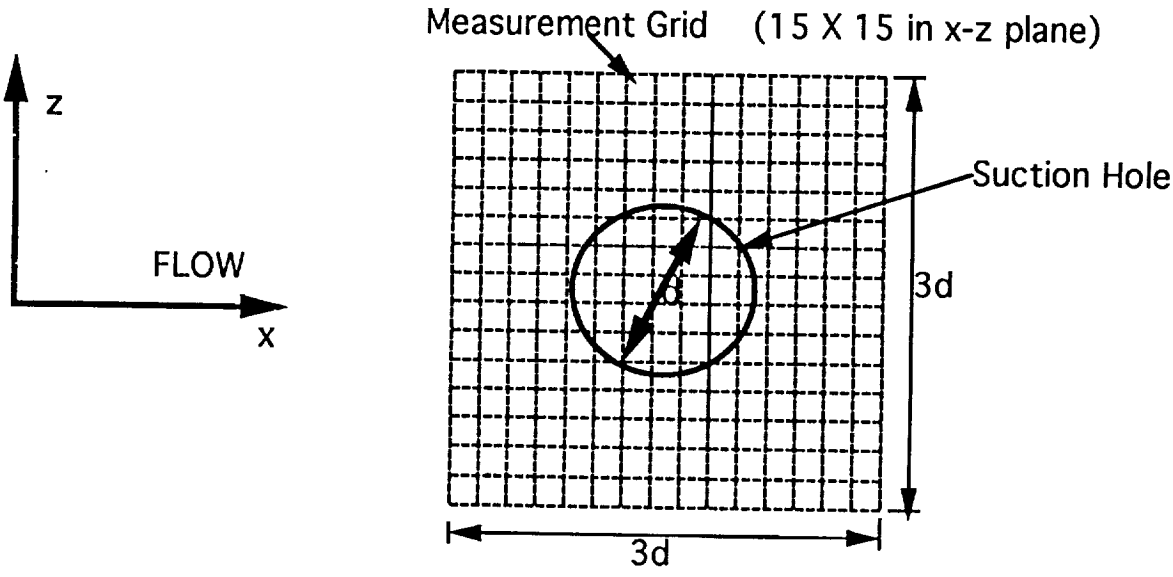

Figure 5. Velocity survey mapping region.